Available online at www.sciencedirect.com
ScienceDirect
Materials Science and Engineering C xx (2007) xxx–xxx
MATERIALS SCIENCE & ENGINEERING C
www.elsevier.com/locate/msec

Two-stage photobioreactor process for the metabolic insertion of nanostructured germanium into the silica microstructure of the diatom *Pinnularia* sp.

Clayton Jeffryes [a], Timothy Gutu [b], Jun Jiao [b], Gregory L. Rorrer [a,*]

[a] *Department of Chemical Engineering, Oregon State University, Corvallis, OR 97331, USA*
[b] *Department of Physics, Portland State University, Portland, OR 97207, USA*

Received 10 August 2006; received in revised form 18 December 2006; accepted 4 January 2007

Abstract

There is significant interest in imbedding nanoscale germanium (Ge) into dielectric silica for optoelectronic applications. In this study, a bioreactor process was developed to metabolically insert nanostructured Ge into a patterned silica matrix of the diatom *Pinnularia* sp. at levels ranging from 0.24 to 0.97 wt.% Ge. In Stage I, the diatom cell culture was grown up to silicon starvation. In Stage II, soluble silicon and germanium were co-fed to the silicon-starved culture to promote one cell division during Ge uptake. In Stage II, soluble Si and Ge were transported into the silicon-starved diatom cell by a surge uptake process, and Ge uptake preceded its incorporation into the frustule. STEM–EDS line scans of the frustule in the newly-divided cells revealed that the Ge was uniformly incorporated into the biosilica. The overall shape of the new frustule was intact, but Si–Ge oxides filled the frustule areolae and altered their nanoscale pore size and geometry. Ge-rich pockets imbedded within the silica frustule and Ge-rich nanoparticles littering the frustule surface were also found. These results suggest that a two-stage diatom cultivation process can biologically fabricate and self-assemble new types of Ge–Si nanocomposite hierarchical materials that possess intricate submicron features.

Keywords: Bioreactor; Biogenic silica; Diatoms; Si–Ge nanocomposites

1. Introduction

Currently, there is significant interest in imbedding nanoscale germanium (Ge) into dielectric silica for optoelectronic applications and nonvolatile memory device structures [1]. For example, nano-crystalline Ge and Ge oxides in silica possess strong blue photoluminescence [2]. Current methods for imbedding germanium into silica (SiO_2) rely on top-down, low-throughput approaches operating at extremes of temperature, such as ion implantation [3], laser ablation [4] or magnetron sputtering [5]. In general, it is extremely difficult to fabricate nanostructured complimentary metal oxide (CMOS) semiconductor materials and at the same time integrate these materials into patterned nanoscale device features needed for the next generation of optoelectronic devices. To address these limitations, biologically-inspired or biomolecule-mediated fabrication techniques are increasingly becoming recognized a new platform for the bottom-up synthesis of nanostructured materials and their self-assembly into hierarchical structures, including metal oxide semiconductors [6–8].

Diatoms are a prolific class of single-celled algae that take up soluble silicon to make silica shells or frustules possessing intricate submicron and nanoscale structures such as patterned pore arrays. Diatoms have been touted as the paradigm for the biofabrication of nanostructured silica [9,10], and many applications of the emerging fields of "diatom nanotechnology" and "silicon biotechnology" have been proposed [11–15]. Several elegant studies have deduced the structure and function of the silaffin class of diatom proteins and peptides that promote the condensation of soluble silicon to silica [16–22]. Unfortunately, biomimetic synthesis of silica promoted these biomolecules has not yet

* Corresponding author. Tel.: +1 541 737 3370; fax: +1 541 737 4600.
E-mail address: rorrergl@engr.orst.edu (G.L. Rorrer).

0928-4931/$ - see front matter © 2007 Elsevier B.V. All rights reserved.
doi:10.1016/j.msec.2007.01.002

duplicated the nanostructure and intricate submicron structure of the diatom frustule, although a top-down writing technique could be used to pattern some of its microscale features [23]. It is our belief that the living diatom itself could be harnessed as a cell factory for massively-parallel fabrication of nanoscale hierarchical metal oxide materials that are packaged into a frustule-like form factor. There is considerable need for this approach, as it has recently been shown that intact diatom frustules act as photonic crystals [24], optical sensors [25], possess weak green photoluminescence [26], and can serve as templates for bioclastic materials processing [27] or nanoparticle assembly [28].

The controlled metabolic insertion of germanium into the silica frustule may produce a Si–Ge nanocomposite imbedded into the frustule microstructure. This Si–Ge nanocomposite could impart optoelectronic properties to this microstructure and at the same time controllably alter the microstructure. In a preliminary study, we cultivated the marine diatom *Nitzschia frustulum* in the presence of soluble germanium. Thermal annealing of the diatom cell mass in air at 800 °C yielded a crystalline white solid consisting of silicon oxide nanoclusters enriched in germanium and calcium oxides [29]. This current study focuses on harnessing the diatom cell growth cycle for the biological fabrication of Si–Ge oxide nanocomposites within the biogenic frustule microstructure.

A two-stage bioreactor process will provide the level of control needed to incorporate the desired composition of germanium into the silica frustule. In Stage I, the diatom cell suspension is grown up to silicon starvation. In Stage II, soluble silicon and germanium are co-fed to the silicon-starved culture to promote *one cell division* while the germanium is being taken up by the organism. With regards to hierarchical structure, pennate diatoms in genus *Pinnularia* are an excellent model organism for biofabrication, as the frustule possesses levels of order spanning the micron, submicron, and nanoscale [30,31].

The first objective of this study was to characterize the cell growth and metal uptake parameters for the two-stage photobioreactor cultivation of *Pinnularia* sp. as a function of Stage II initial germanium concentration. The second objective was to determine if metabolically inserted germanium was nanostructured within the biogenic silica. Towards this end, frustules were isolated by aqueous hydrogen peroxide treatment at room temperature to preserve the biogenic silica structure. The third objective was to assess if metabolic insertion of germanium could controllably alter the frustule microstructure. Based upon these results, a conceptual model for metabolic insertion of germanium into frustule by the two-stage cultivation process was proposed. Evaluation of optoelectronic material properties was beyond the scope of this study.

2. Experimental

2.1. Cell culture

Pure cultures of the marine diatom *Pinnularia* sp. (Ehrenberg) were obtained by the UTEX Culture Collection of Algae (UTEX# B679). *Pinnularia* sp. [31] is a photosynthetic diatom possessing pennate morphology, with a nominal length of 30 μm and width of 5 μm. Stock cultures of *Pinnularia* sp. were maintained on enriched natural seawater medium without agitation in 500 mL foam-stoppered flasks (80 mL per flask) under cool white fluorescent light at 50 $\mu E/m^2$-s incident light flux intensity and photoperiod of 14 h light/10 h dark within an incubator set at 22 °C. The cell suspension was subcultured every 14 days at 10% v/v. The typical cell density just before subculture was $\sim 1 \cdot 10^6$ cells/mL. Filtered, UV-sterilized natural seawater was obtained from the Hatfield Marine Science Center, Newport, Oregon, and re-filtered at 5 μm. The enrichment medium, a modified LDM recipe, (http://www.zo.utexas.edu/research/utex/media/ldm.html) was designed for silicon-limited culture growth with an N:P ratio of 23.4:1. Macronutrients in the enrichment medium were 5.125 mM $NaNO_3$, 0.0543 mM $K_2HPO_4 \cdot 3H_2O$, 0.165 mM KH_2PO_4, 1.03 mM $Na_2SiO_3 \cdot 5H_2O$; micronutrient metals were 69.6 μM $MgSO_4 \cdot H_2O$, 3.08 μM $FeSO_4 \cdot 7H_2O$, 1.77 μM $MnCl_2 \cdot 4H_2O$, 0.314 μM $ZnCl_2$, 0.072 μM $CoCl_2 \cdot 6H_2O$, 0.136 μM $(NH_4)_6Mo_7O_{24} \cdot 4H_2O$, 17.2 μM Na_2EDTA; vitamins were 0.013 μM B_{12}, 0.07 μM biotin, 5.1 μM thiamine HCl, 13.6 μM thymine, 7.2 μM Ca-pantothenate, 1.25 μM *p*-aminobenozic acid, 95 μM *meso*-inositol, 13.9 μM nicotinic acid. The final medium was autoclaved at 121 °C for 30 min. All culture manipulations were performed in a laminar flow hood using sterile technique.

2.2. Photobioreactor design

The bubble-column photobioreactor shown in Fig. 1 was used to cultivate the *Pinnularia* sp. photosynthetic cell suspension under controlled conditions. The bioreactor vessel was a glass column of 10.5 cm inner diameter, 4.8 mm wall thickness, and 70.5 cm height to provide a total volume of 6.1 L and working

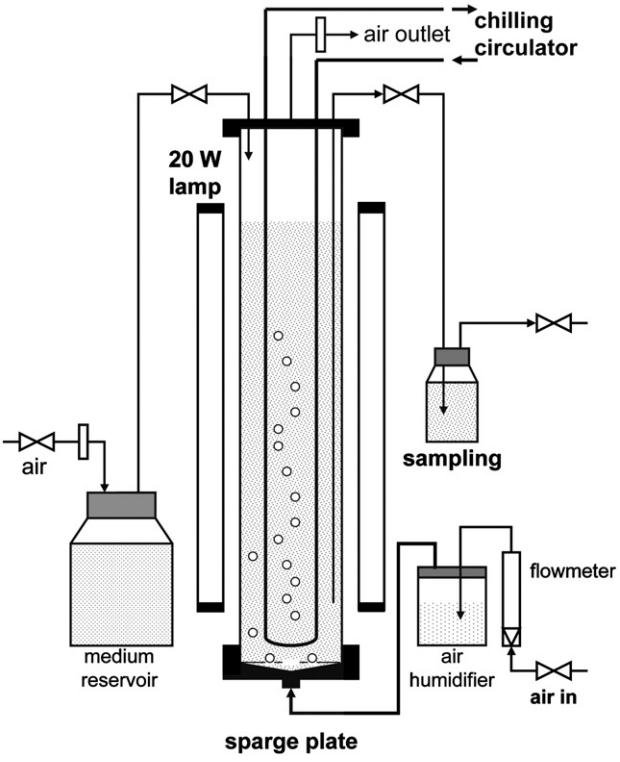

Fig. 1. Schematic of bubble-column photobioreactor.

volume of 3.9 L (45 cm). The glass column was mounted onto two stainless steel support plates at the base and top. The baseplate assembly contained a stainless steel sparger plate consisting of four 1.0 mm diameter holes on a 3.6 cm square pitch. Pressurized house air was particulate filtered, metered through a flowmeter, sterile filtered at 0.2 μm, and introduced to the baseplate. The headplate assembly contained 8 ports, including a fresh medium delivery port, thermocouple port, a 4.6 mm inner diameter sampling tube, 11 mm D.O. electrode port, two air outlet ports, and 9.5 mm outer diameter by 1.09 m length stainless steel internal U-tube heat exchanger. Controlled sampling of the liquid suspension within the vessel was accomplished by pressurizing the vessel headspace and collecting the liquid in a sterile culture bottle. Water from a temperature-controlled chilling circulator was pumped through the internal heat exchanger to provide constant temperature within the bioreactor vessel. The bioreactor was externally illuminated by six 20 W cool white fluorescent lamps of 57 cm length vertically positioned around the glass vessel in a hexagonal array about 1–2 cm from the vessel surface. The lamps were connected to a photoperiod timer. The incident light flux intensity was measured with a LI-COR SA 190 PAR quantum sensor positioned at the interior surface and pointed towards the light source at 6 radial positions and 3 axial positions (top, middle, bottom). Detailed process conditions used in this study are provided in Table 1. Four identical photobioreactor systems were operated in parallel.

2.3. Two-stage photobioreactor cultivation

In all bioreactor experiments, medium composition was the same as for the *Pinnularia* sp. flask cultures with the exception of the dissolved silicon concentration. The medium and bioreactor were autoclaved separately. The bioreactor was inoculated using 17 day old *Pinnularia* sp. flask cultures by sterile transfer of a defined inoculum volume. In Stage I of the two-stage photobioreactor cultivation process, culture growth was designed for silicon limitation. The target initial cell density was $7.5 \cdot 10^4$ cells/mL, the initial pH was 8.3, and the initial dissolved silicon concentration ($C_{\mathbf{Si,o}}$) was 0.53 mmol Si/L (as soluble Na_2SiO_3), to provide a target final cell number density of $6.0 \cdot 10^5$ cells/mL, or approximately 3 cell divisions. The photoperiod was set to 4 h illumination, then 10 h dark, then 14 h illumination/10 h dark for the rest of the cultivation period. After all the soluble silicon was consumed, the culture was kept in a silicon-starved state at constant, stationary phase cell density for at least 24 h. At the point of silicon starvation, Stage II of cultivation was initiated 4 h into the photoperiod. Specifically, defined volumes of 100 mmol Na_2SiO_3/L and 5.0 mmol GeO_2/L stock solutions in de-ionized water were mixed together and then injected into the bioreactor culture. The initial dissolved silicon concentration was always reset to 0.53 mmol/L, which was enough silicon to provide for one more cell division of silicon-starved cell culture leading to a final cell number density of $1.2 \cdot 10^6$ cells/mL at the end of Stage II. In Stage II, the initial soluble germanium concentration varied from 0, 4.25, 17.3, 25.2 to 38.3 μmol/L at the fixed initial Si concentration of 0.53 mmol/L, to provide initial Si:Ge molar ratios ranging from 125:1 to 14:1 (initial Si:Ge mass ratios from 48:1 to 5.4:1). The cultivation times for Stages I and II were 114 and 56 h respectively (170 h total).

During Stage I, 40 mL of the cell suspension was sampled at 12 h intervals for determination of cell number density, pH, and dissolved silicon concentration. During Stage II, the culture suspension was sampled 8 times during the first 12 h for cell number density, pH, dissolved silicon concentration, dissolved germanium concentration, and then once every 12 h thereafter. Additionally, at 0, 12, and 56 h of Stage II cultivation, 540 mL samples were taken for determination of silicon and germanium content in the dry cell biomass (Y_{Si}, Y_{Ge}), isolation of intact frustules for nanoscale analysis by SEM, TEM, STEM–EDS, and elemental composition of germanium and trace minerals in the silica frustule.

Table 1
Summary of process conditions for two-stage photobioreactor cultivation of *Pinnularia* sp.

Process parameter		Stage I	Stage II
Target initial conditions			
Cell number density	$X_{N,o}$	$7.5 \cdot 10^4$ cells/mL	$6.0 \cdot 10^5$ cells/mL
Initial silicon concentration	$C_{Si,o}$	0.53 mmol Si/L	0.53 mmol Si/L
Initial germanium concentration	$C_{Ge,o}$	0.0 mmol Ge/L	0.0 μmol Ge/L (control) 4.25–38.3 μmol Ge/L
	$C_{Si,o}/C_{Ge,o}$		125–14 (mole basis) 49–5.4 (mass basis)
Process conditions			
Temperature	T	22 °C	22 °C
Initial culture volume	V_o	3.90 L	3.04 L
Incident light intensity	I_o	149 ± 15 μE/m^2-s	149 ± 15 μE/m^2-s
Fractional photoperiod	f	0.583 (14 h light/10 h dark)	0.583 (14 h light/10 h dark)
Aeration rate	v_g	0.65 L air L^{-1} min^{-1}	0.83 L air L^{-1} min^{-1}
CO_2 partial pressure	P_{CO_2}	350 ppm (ambient air)	350 ppm (ambient air)
Cultivation time	t	114 h	56 h

2.4. Culture suspension assays

To determine cell number density (X_N, #cells/mL) a 0.1 mL sample of the cell suspension was diluted in 10.0 mL of Isoton II electrolyte solution (Beckman-Coulter). Cells were counted on Beckman Z2 Coulter Counter at a threshold of 8 μm (duplicate assay). To determine soluble silicon and germanium concentrations, immediately after sampling, a 30 mL sample aliquot of cell suspension was syringe filtered with a cellulose ester membrane (3.0 μm pore size, 25 mm diameter). Soluble silicon concentration (C_{Si}, mmol Si/L) in the filtrate was determined by spectrophotometric assay at 360 nm following derivatization of a 5.0 mL liquid sample aliquot with 0.2 mL of 13.3% w/v ammonium molybdate reagent in water and 0.1 mL 18.7% v/v HCl in water as described by Fanning and Pilson [32]. The

Please cite this article as: C. Jeffryes et al., Mater. Sci. Eng. (2007), doi:10.1016/j.msec.2007.01.002

soluble germanium concentration (C_{Ge}, μmol Ge/L) in the filtrate was determined by spectrophotometric assay at 510 nm following derivatization of a 1.0 mL liquid sample with 1.0 mL of 0.01% w/v phenylfluorone reagent in methanol, 1.7 mL of 10% v/v HCl in water, 0.3 mL of 24% w/v H_2SO_4 in water, and 1.0 mL buffer (3.3 M sodium acetate in 5.8 N acetic acid) as described by Luke and Campbell [33] and Marczenko [34]. All Si and Ge concentration assays were performed in duplicate. For assay of dry cell mass, a 90 mL aliquot of cell suspension was centrifuged at 4000 rpm (2000 ×*g*) for 10 min. The supernatant was drawn off, the pellet was suspended in 45 mL de-ionized water and centrifuged again; this washing step was repeated two more times to completely remove soluble salts. The washed pellet was transferred to an aluminum weighing dish, weighed, oven dried in air at 80 °C for 24 h, and then weighed after drying.

2.5. Si and Ge content in cell mass

The silicon and germanium content in the cell mass was determined after fusion with molten NaOH. A 20 mg aliquot of dry biomass was weighed to precision of 0.1 mg and then added to 1.0 g solid NaOH in a zirconium crucible. The mixture was heated to 400 °C within a furnace in air for 25 min. After cooling, the NaOH-fused sample was dissolved in 20 mL de-ionized H_2O and then neutralized to pH 7.0 with 1.4 M HNO_3. The neutralized solution was spectrophotometrically assayed for soluble Si and Ge concentration as described above, and the amount of Si and Ge in the biomass was determined from these concentration values, the total volume of neutralized solution, and the original dry cell mass.

2.6. Intact frustule isolation

Intact silica frustules were prepared by hydrogen peroxide treatment. The procedure was designed to minimize frustule breakage due to drying and mixing of the sample. Specifically, a 100 mL aliquot of the culture suspension sampled from the bioreactor was allowed to settle in a 200 mL sealed glass bottle for 6 h. About 90 mL of supernatant was removed with a pipette, and the dense cell slurry was re-suspended in 100 mL de-ionized water and then allowed to settle again. The supernatant was removed with a pipette, leaving behind about 10 mL of dense cell suspension in de-ionized H_2O. The cell suspension was transferred to a 50 mL centrifuge tube. To initiate the oxidation of organic materials in the cell mass, 30 mL of 30 wt.% aqueous hydrogen peroxide (H_2O_2) was added to the tube, along with 0.2 mL of 37 wt.% HCl to lower the pH to 2.5 for removal of carbonates. The oxidation reaction was unmixed at room temperature for at least 48 h. During this time the cell mass color changed from yellow-green to white. The uncapped centrifuge tube and contents were degassed under vacuum at room temperature for 1.0 h, which removed oxygen bubbles and allowed the hydrogen peroxide treated cell mass to settle. The degassed supernatant was pipetted from the white particle slurry. The slurry was re-suspended in 30 mL MeOH and allowed to settle. The supernatant was removed by pipette, and the MeOH washing procedure was repeated two more times to completely remove water. The frustules, white in color, were stored at 4 °C in 10 mL MeOH within a sealed glass vial.

2.7. ICP analysis of frustules

A 5–10 mg aliquot of the frustule suspension in MeOH described above was dried in air. The solid mass was weighed to precision of 0.1 mg and then subjected to the NaOH fusion procedure described above. A 20 mL aliquot of the final solution was then assayed for Si, Ge, Ca, and Mg by ion-coupled plasma (ICP) analysis using a Varian (Liberty 150) ICP emission spectrometer. The analysis wavelengths were 251.611 (Si), 265.118 nm (Ge), 279.553 nm (Mg) and 393.366 nm (Ca). Limits of detection for Si, Ge, Ca, and Mg in the assay solution were 0.07, 0.04, 0.01, 0.04 mg/L respectively.

2.8. Electron microscopy

Pinnularia sp. frustules isolated by hydrogen peroxide treatment were analyzed by scanning electron microscopy (SEM) using an FEI Sirion field emission SEM and by transmission electron microscopy (TEM) using an FEI Tecnai F20 high resolution TEM (200 keV) equipped with embedded scanning transmission electron microscopy (STEM) and an X-ray energy dispersive analysis (EDS) probe. For SEM analyses, about 20 μL of the frustule suspension in methanol (diluted 10:1 v/v) was pipetted onto a carbon tape affixed to an aluminum stub. The sample was not coated with a conductive carbon layer. To avoid surface charging, the FESEM was operated at a low acceleration voltage of 2 keV. For TEM and STEM–EDS analyses, about 20 μL of frustule suspension in methanol (diluted 10:1 v/v) was pipetted onto a Holey carbon copper TEM grid (Electron Microscopy Services HC300-Cu, 3.05 mm diameter, 300 mesh, 54 μm hole width, 31 μm bar width). As the methanol evaporated to dryness, about 2–5 frustules per square were randomly dispersed onto the TEM grid. EDS elemental line scans were acquired in STEM mode (200 keV, tilt angle of 15°) with sampling increment dependent on the length of the line scan (24 sample points if line was <500 nm, 49 sample points if line was >500 nm, 5000 ms per sample point). Characteristic Kα energy peaks (all keV) were identified as 0.52 (O), 1.25 (Mg), 1.74 (Si), 3.69 (Ca), 9.86 (Ge, $K\alpha_1$), 9.88 (Ge,$K\alpha_2$). The calibrated peak intensity calibration factors for atomic composition analysis (k-factors) normalized to silicon were 1.980 (O), 1.034 (Mg), 1.148 (Ca), and 2.192 (Ge).

3. Results

3.1. Two-stage bioreactor cultivation

A two-stage photobioreactor cultivation process incorporated germanium into the silica frustule of the photosynthetic marine diatom *Pinnularia* sp. In Stage I, soluble silicon was added to the cell suspension culture, and the culture was grown

Please cite this article as: C. Jeffryes et al., Mater. Sci. Eng. (2007), doi:10.1016/j.msec.2007.01.002

Table 2
Comparison of photobioreactor performance parameters for two-stage cultivation of *Pinnularia* sp.

Growth parameter	Stage	Initial germanium concentration in Stage II	
		0.0 μmol/L	38.3 μmol/L
Specific growth rate, $\mu/(h^{-1})$ [a]	I	0.0515±0.0084	0.0572±0.0028
	II	0.0656±0.0079	0.0447±0.0041
Cell number yield, $Y_{Xn/Si}$ (#cells/mmol Si) [b]	I	$7.23\cdot10^8\pm1.05\cdot10^8$	$6.60\cdot10^8\pm9.41\cdot10^7$
	II	$1.16\cdot10^9\pm1.28\cdot10^8$	$9.16\cdot10^8\pm5.26\cdot10^7$
Dry cell mass yield, $Y_{X/Si}$ (g DW/mmol Si) [b]	I	0.324±0.0034	0.335±0.0033
	II	0.777±0.064	0.465±0.044
Final cell number density, $X_{N,f}$ (#cells/mL) [b]	I	$5.42\cdot10^5\pm2.04\cdot10^4$	$4.13\cdot10^5\pm3.44\cdot10^4$
	II	$1.17\cdot10^6\pm9.55\cdot10^4$	$8.15\cdot10^5\pm4.50\cdot10^4$

[a] 0–68 h Stage I, 114–125 h Stage I+II (0–11 h Stage II); ±1.0 S.E.
[b] Average from 79–113 h Stage I, 140–170 h Stage I+II (26–56 h Stage II); ±1.0 S.D.

up to silicon starvation. In Stage II, a mixture of soluble silicon and germanium was added to the silicon-starved culture. The cultivation conditions for Stages I and II are provided in Table 1, and the culture growth parameters in each stage for two representative cultivations are summarized in Table 2.

Cell number density and dissolved silicon concentration in the culture medium vs. cultivation time for Stages I and II for the control experiment where no germanium was added to Stage II is presented in Fig. 2a. In Stage I, the amount of silicon added to the culture was designed to accomplish three cell doublings, so that at an initial cell number density of $7.5\cdot10^4$ cells/mL, and final cell number density was nominally $6.0\cdot10^5$ cells/mL. In Stage I of cultivation, silicon consumption was growth associated, and the cell number density increased proportionally to the decrease in dissolved silicon concentration with time. When all the dissolved silicon in the culture medium was consumed, the cell number density leveled off and then became constant with time. Silicon starvation was defined as a culture state where the cell number density was constant and the dissolved silicon concentration was zero for at least one photoperiod (24 h). In Stage I of cultivation, the pH rose from 8.3 at inoculation to 9.0 at the end of stationary phase. In Stage II of cultivation, soluble silicon was added to the silicon-starved culture at 4 h into the 14 h light portion of the 24 h (14 h light/10 h dark) photoperiod, and the cultivation was allowed to proceed for an additional 56 h. The amount of silicon added to the Stage II culture provided for one more cell number doubling. In Stage II, surge uptake of silicon was observed, where most of the dissolved silicon was taken up by the culture

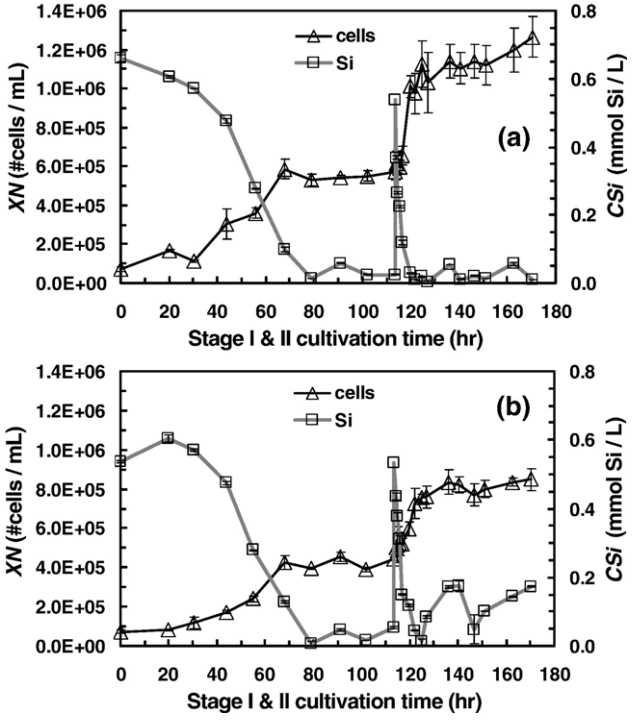

Fig. 2. Cell number density (X_N) and soluble Si concentration in culture medium (C_{Si}) vs. time for two-stage photobioreactor cultivation of the marine diatom *Pinnularia* sp. Stage II initial concentrations of (a) 0.0 μmol Ge/L and 0.53 mmol Si/L; (b) 38 μmol Ge/L and 0.53 mmol Si/L.

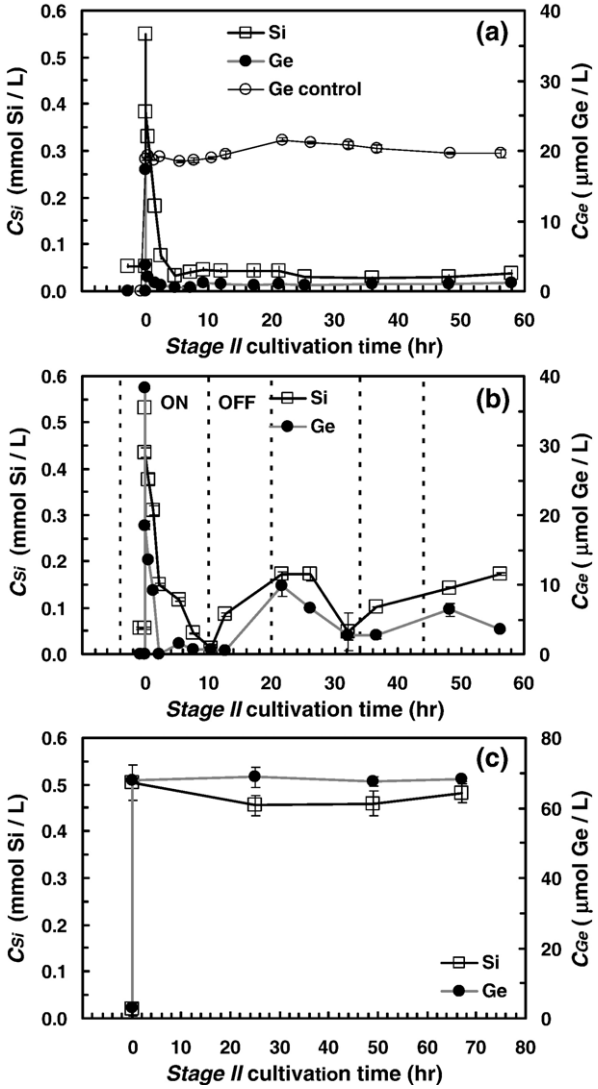

Fig. 3. Effect of initial soluble Si and Ge concentration on Si and Ge uptake from the culture medium during Stage II of cultivation. (a) 17 μmol Ge/L and 0.55 mmol Si/L (initial Si:Ge molar ratio of 32:1); (b) 38 μmol Ge/L and 0.53 mmol Si/L (initial Si:Ge molar ratio of 14:1); (c) 69 μmol Ge/L and 0.48 mmol Si/L (initial Si:Ge molar ratio of 7:1).

Please cite this article as: C. Jeffryes et al., Mater. Sci. Eng. (2007), doi:10.1016/j.msec.2007.01.002

within the remaining 10 h of the first photoperiod. After 12 h, cell doubling was complete, the cell number density leveled off, and the culture was considered silicon starved once again.

Cell number density (X_N) and dissolved silicon concentration (C_{Si}) in the culture medium vs. cultivation time for Stages I and II for the control experiment where 38 μmol/L of soluble germanium and 0.53 mmol/L soluble silicon were co-added to Stage II is presented in Fig. 2b. After 38 μmol/L of soluble Ge was added to Stage II, the cultivation was similar to the control with no germanium.

3.2. Silicon and germanium uptake

Profiles of dissolved silicon and germanium concentration (C_{Ge}) vs. cultivation time during Stage II at initial Ge concentrations of 17 and 38 μmolGe/L are presented in Fig. 3. During the first 10 h of Stage II, soluble Ge uptake by the diatom cell suspension culture was commensurate with the surge uptake of soluble Si. At the initial soluble germanium concentration of 17 μmol/L, the dissolved germanium and silicon concentrations in the medium remained at zero after the initial surge uptake. However, at the higher initial soluble germanium concentration of 38 μmol/L, the concentration of soluble Ge and Si did not stay at zero but instead cycled up and down in a pattern commensurate with the photoperiod. Specifically, when the lights were off, some Si and Ge were released back into the liquid medium. However, when the lights came back on, both the Si and Ge were taken up once again. Finally, there was a limit to Ge uptake based on the initial molar ratio of Si:Ge in Stage II. At a Stage II initial Ge concentration of 69 μmol/L (initial Si:Ge molar ratio of 7:1), there was no uptake of either soluble silicon and germanium (Fig. 3c) and no cell division was observed. Control experiments with no cells at an initial Ge concentration of 20 μmol /L confirmed that Ge did not adsorb onto the surfaces of the bioreactor (Fig. 3a).

3.3. Solid analysis of bioreactor-cultured cells

The silicon content in the dry cell mass at the end of Stage II for each photobioreactor experiment is presented in Fig. 4a. The germanium content within the dry cell biomass at Stage II cultivation times of 12 h and 56 h is compared in Fig. 4b for Stage II initial Ge concentrations of 17, 25 and 38 μmol/L. The silicon content in the dry cell mass was stable as the germanium content in the cell mass increased.

Elemental (ICP) analysis of Ge in the silica frustules isolated hydrogen peroxide treatment of the cell suspension obtained at two Stage II cultivation times of 12 and 56 h is presented in Fig. 4c at Stage II initial germanium concentrations ranging from 0 (control) to 38 μmol/L. The hydrogen peroxide treatment was designed to gently oxidize organic materials away from the insoluble silica frustule. Only 14–15 wt.% of the total dry cell mass remained insoluble after hydrogen peroxide treatment (Table 3), and this inorganic solid yield was not affected by the initial concentration of Ge in Stage II. Errors in the elemental analysis reflected the errors incurred during the hydrogen peroxide treatment step, not the ICP analysis. Residual calcium

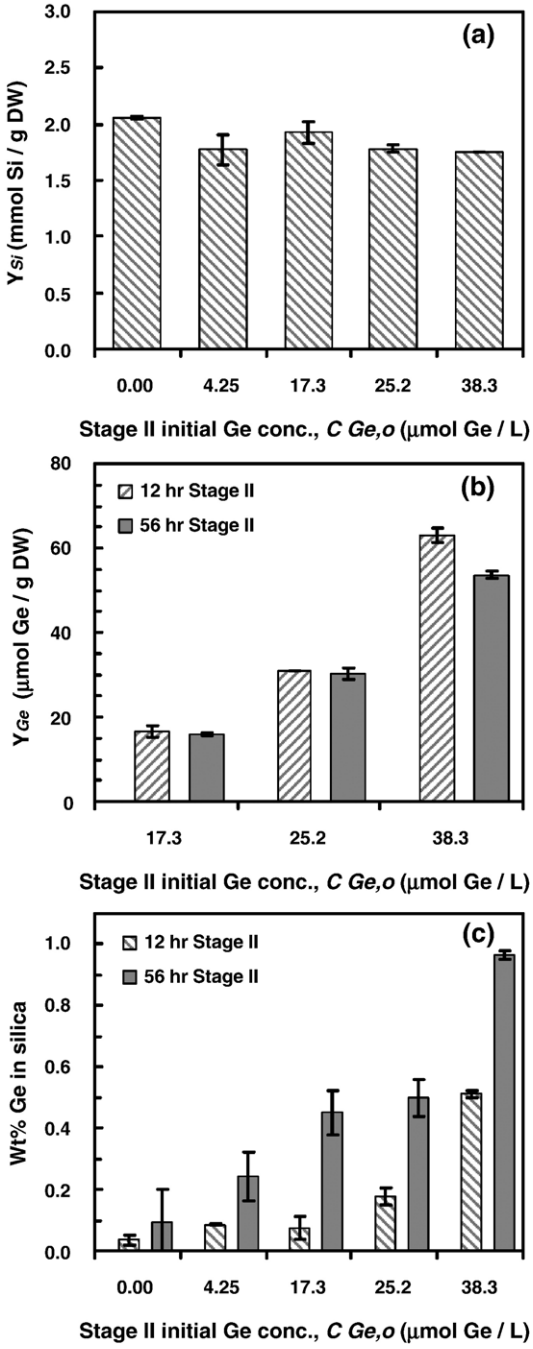

Fig. 4. Effect of Stage II initial Ge concentration on Si and Ge concentration in solid. Initial Ge concentrations ranged from 4.25 to 38.3 μmol /L to provide initial Si:Ge molar ratios ranging from 125:1 to 14:1. (a) Si content in cell biomass (Y_{Si}, mmol Si/g DW) at Stage II cultivation time of 56 h; (b) Ge content in cell biomass (Y_{Ge}, μmol Ge/g DW) at Stage II cultivation times of 12 and 56 h; (c) Ge content in hydrogen peroxide treated silica frustule (wt.% Ge in silica) at Stage II cultivation times of 12 and 56 h.

(Ca) and magnesium (Mg) remained in the frustule after hydrogen peroxide treatment, with compositions ranging 0.10 to 0.25 wt.% (Table 3). From material balance studies conducted on the hydrogen peroxide treatment step, only about 36±4.7% of the Ge initially in the cell mass sample still remained within the intact silica frustule; the rest of the Ge dissolved during hydrogen peroxide treatment and was recovered in the washings. The Ge

Please cite this article as: C. Jeffryes et al., Mater. Sci. Eng. (2007), doi:10.1016/j.msec.2007.01.002

Table 3
ICP analysis of metal content in silica frustules isolated by hydrogen peroxide treatment of *Pinnularia* sp. cell mass containing metabolically inserted germanium

Stage II		Initial germanium concentration in Stage II				
Time (h)		0.0 μmol/L	4.25 μmol/L	17.3 μmol/L	25.2 μmol/L	38.3 μmol/L
12 [a]	Ge (wt.%)	0.036±0.017	0.085±0.0015	0.075±0.038	0.178±0.027	0.511±0.012
	Ca (wt.%)	0.169±0.084	0.036±0.044	0.230±0.176	0.009±0.022	0.032±0.021
	Mg (wt.%)	0.132±0.034	0.167±0.027	0.213±0.105	0.177±0.020	0.160±0.013
56 [a]	Ge (wt.%)	0.092±0.110 [b]	0.243±0.081	0.452±0.072	0.498±0.061	0.965±0.012
	Ca (wt.%)	0.247±0.149	0.140±0.026	0.053±0.038	0.086±0.033	0.092±0.131
	Mg (wt.%)	0.142±0.036	0.134±0.022	0.111±0.022	0.108±0.032	0.106±0.017
0–56 [c]	g H_2O_2 solid/g DW	0.156±0.046	0.158±0.030		0.144±0.023	0.159±0.060

[a] ±1.0 S.D for $n=3$ samples (3× replicates per sample).
[b] Analyses near ICP detection limit for Ge.
[c] Average (±1.0 S.D.) from Stage II cultivation times of 0, 12, 36, and 56 h ($n=4$ with 2 replicates per sample).

contents of the frustules were very consistent, particularly for photobioreactor experiments conducted at Stage II initial Ge concentrations of 17 and 38 μmol/L, where the frustule germanium content ranged from 0.452±0.072 to 0.965±0.012 wt.% after 56 h of Stage II cultivation. A small amount of germanium was also detected by ICP in the control sample (initial concentration of 0.0 μmol/L Ge added to Stage II), but within the limits of detection error, the Ge content was zero. The Ge content in the frustule after 12 h of Stage II cultivation was consistently about two times smaller than the germanium content after 56 h. In contrast, the Ge content in the dry cell biomass *before* hydrogen peroxide treatment was nominally the same after 12 and 56 h.

3.4. SEM analysis of frustule morphology before Ge addition

Scanning electron microscopy (SEM) of representative frustules obtained by hydrogen peroxide treatment of *Pinnularia* sp. cell biomass obtained from the end of the Stage I of the photobioreactor cultivation (114 h) is presented in Fig. 5. SEM images revealed the frustules were intact, and possessed levels of order spanning the micron and submicron (100–1000 nm) scales. The aqueous hydrogen peroxide treatment procedure did not always break apart the frustule into its upper *epi*-valve and lower *hypo*-valve; both were visible in Fig. 5a.

3.5. TEM analysis of submicron frustule morphology with and without germanium

Frustules of the marine diatom *Pinnularia* sp. were prepared from hydrogen peroxide treatment of cell biomass generated by a two-stage bioreactor cultivation process described above. TEM images of a representative *Pinnularia* sp. frustule obtained from cell biomass cultivated on silicon with no germanium after 56 h of Stage II cultivation are shown in Fig. 6a, b, and c at micron, submicron (100–1000 nm) and nanoscale (1–100 nm) respectively. A strip of thickened silica called a *raphae* ran axially down the length of the frustule (Fig. 6a). Lateral ribs (*costae*) ran perpendicular to the *raphae* at 200 nm intervals (Fig. 6b). The *costae* formed rows of ~200 nm *areolae*, each of which possessed a "bottom" of thin silica containing a concentrically-arranged array of 5–10 smaller pores called *velum* (Fig. 6c).

In subsequent experiments, a mixture soluble silicon and germanium were added to the culture to initiate Stage II of the cultivation. TEM images of a representative *Pinnularia* sp. frustule obtained from hydrogen-peroxide treated cell mass containing 0.96 wt.% germanium (56 h of Stage II cultivation) are presented in Fig. 6d, e, and f at the micron, submicron, and nanoscale respectively. EDS elemental analysis confirmed that the frustule itself now contained germanium, with a distinct $K\alpha_{1,2}$ peaks for Ge at 9.86–9.89 keV. The incorporation of germanium into the biogenic silica altered frustule morphology. Although the overall shape of the frustule containing 0.96 wt.% Ge was not changed (Fig. 6d), the raphae thickened (Fig. 6e). The lateral ribs (*costae*) also thickened and assumed a wavy shape. Although pore arrays were still observed, they were not always linear (Fig. 6f). The *areolae* filled in with silica, and the *velum* partially fused together to form pores of 50 to 100 nm nominal diameter.

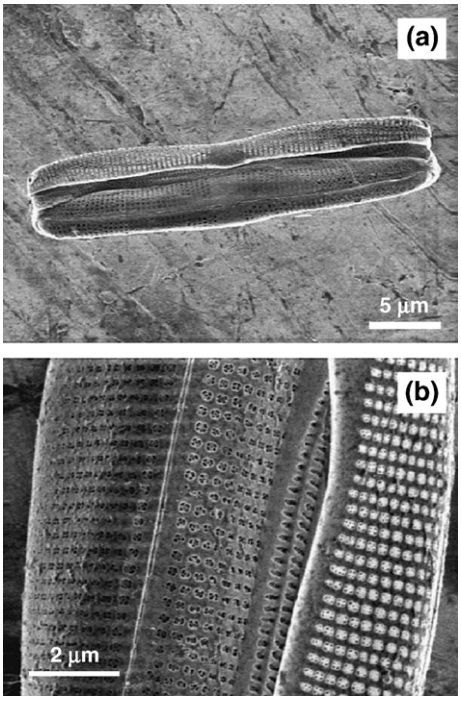

Fig. 5. SEM image of intact silica frustule of *Pinnularia* sp. obtained at the end of Stage I cultivation. (a) Side (girdle band) view; (b) pore array.

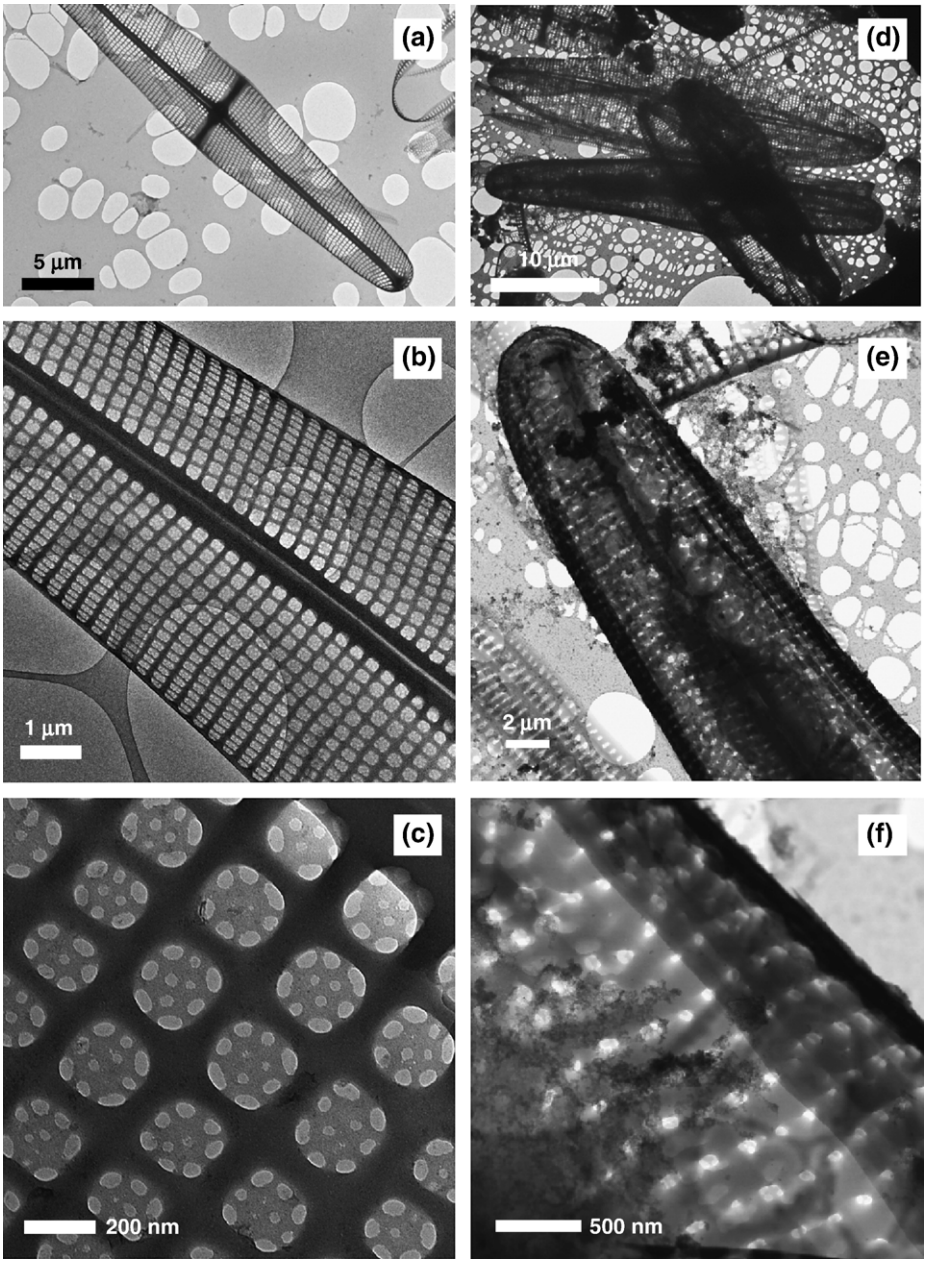

Fig. 6. TEM images of intact silica frustule of *Pinnularia* sp. obtained after 56 h of Stage II cultivation. (a)–(c) Micron, submicron, and nanostructure at Stage II initial concentrations of 0 µmol Ge/L Ge (control) and 0.53 mmol Si/L; (d)–(f) micron, submicron, and nanostructure at Stage II initial concentrations of 38 µmol Ge/L and 0.53 mmol Si /L.

3.6. STEM–EDS analysis of composite nanostructure after germanium addition

STEM–EDS line scans of silicon and germanium were performed on selected submicron features of the frustule in the attempt to identify Si–Ge nanostructures. An elemental line scan running across the entire frustule showed that germanium was present throughout the material (Fig. 7a). The Si and Ge line scans were jagged because the line scan periodically intercepted a pore space. Specific submicron features considered the solid regions across a series of lateral ribs (Fig. 7b), solid region between two pores (Fig. 7c), nanostructures within a single *areolae* (Fig. 7d), and a solid region containing nanoparticles partially filling an *areolae* (Fig. 7e). In general, germanium was dispersed into silica for features at both the submicron (100–1000 nm) and nanometer (1–100 nm) scales. Furthermore, there were several "pockets" of solid material containing elevated levels of germanium or germanium gradients (Fig. 7c). Finally, solid regions with nanoparticle chains were significantly enriched in germanium (Fig. 7e). Putative girdle band structures were also enriched in germanium (Fig. 7f).

EDS was not used to quantitatively estimate the local (nanoscale) atomic composition of the diatom frustule, due to the dominance of the Si signal. However, the calibrated k-factor for the EDS signal intensity of Ge normalized to the signal

Please cite this article as: C. Jeffryes et al., Mater. Sci. Eng. (2007), doi:10.1016/j.msec.2007.01.002

intensity of Si is 2.192, which would provide a measure of local Si:Ge ratios from the Si–Ge line scans in Fig. 7 if desired. Consequently, bulk analysis of Ge by ICP (Table 3) was used to quantify the Ge composition in the diatom biosilica.

4. Discussion

This study is an example of a novel bioprocess engineering strategy that uses living cells as the platform for the biological fabrication of nanostructured metal oxide materials that possess hierarchical structure at the submicron and micron scales. Specifically, we developed a two-stage photobioreactor process for the metabolic insertion of nanostructured germanium into the silica microstructure of the marine diatom *Pinnularia* sp. To provide the context for the results, the diatom cell cycle is briefly overviewed. Each diatom frustule has two *valves* that fit together like a Petri dish (Fig. 8). Just before each diatom cell divides, a new valve (the smaller *hypo*-valve) is formed at the plane of cell division within the silica deposition vesicle, or SDV. Silicon metabolism in the diatom is linked to the four phases of its cell cycle: G1 (photosynthetic growth), S (DNA replication), G2 (Si uptake and new valve formation), and M (mitosis) as reviewed by Martin-Jézéquel et al. [35]. Details of frustule development within diatom cell cycle are described by Kröger and Wetherbee

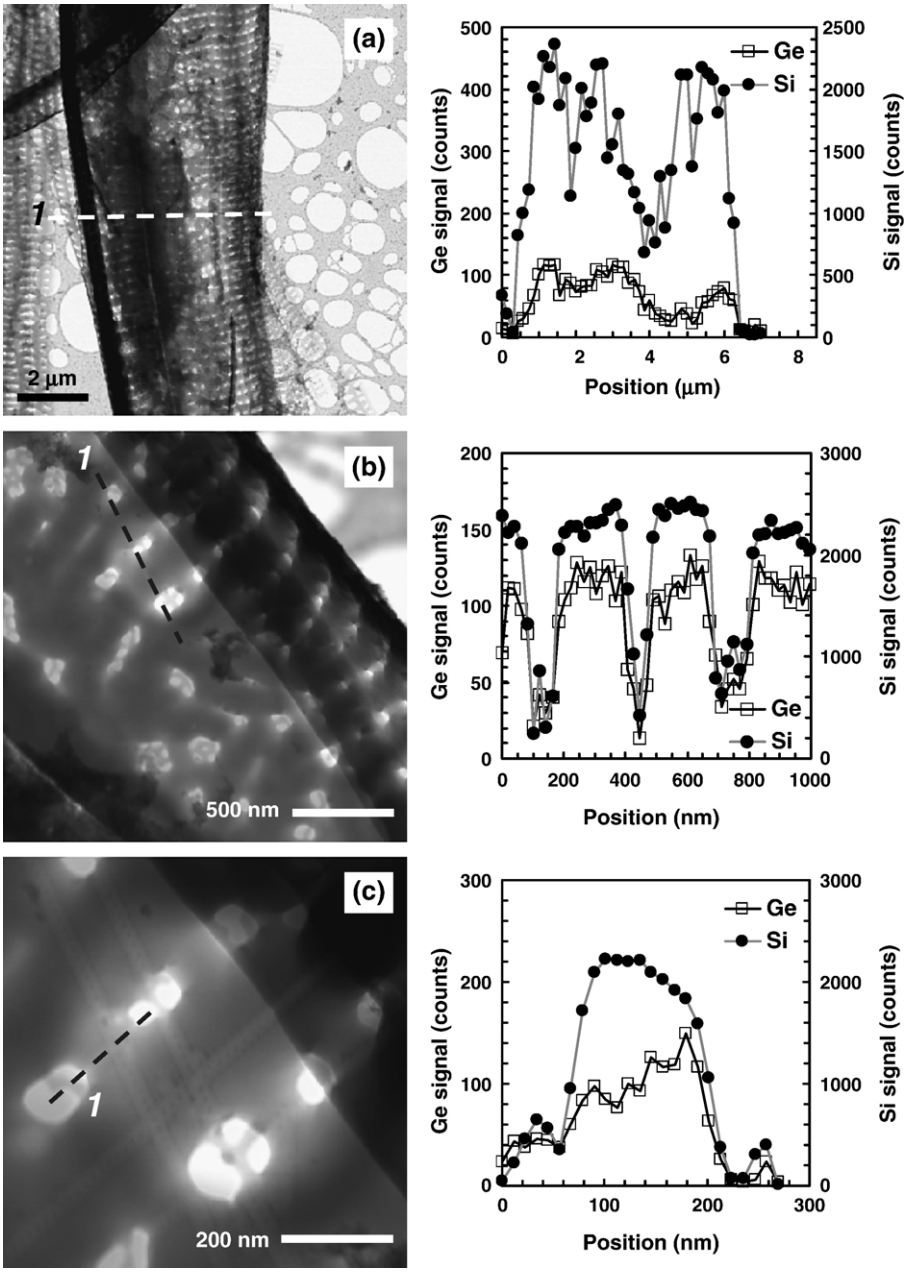

Fig. 7. STEM–EDS analysis of intact silica frustule of *Pinnularia* sp. obtained after 56 h of Stage II cultivation at initial Ge concentration of 38 µmol/L and initial Si concentration of 0.53 mmol/L. STEM image and Si+Ge line scans: (a) across entire frustule; (b) across a series of ribs (*costae*); (c) between two pores; (d) through nanostructure of single *areolae*; (e) through a region containing Ge-rich nanoparticles covering a pore; (f) along the length of a putative girdle band partially separated from its valve.

Please cite this article as: C. Jeffryes et al., Mater. Sci. Eng. (2007), doi:10.1016/j.msec.2007.01.002

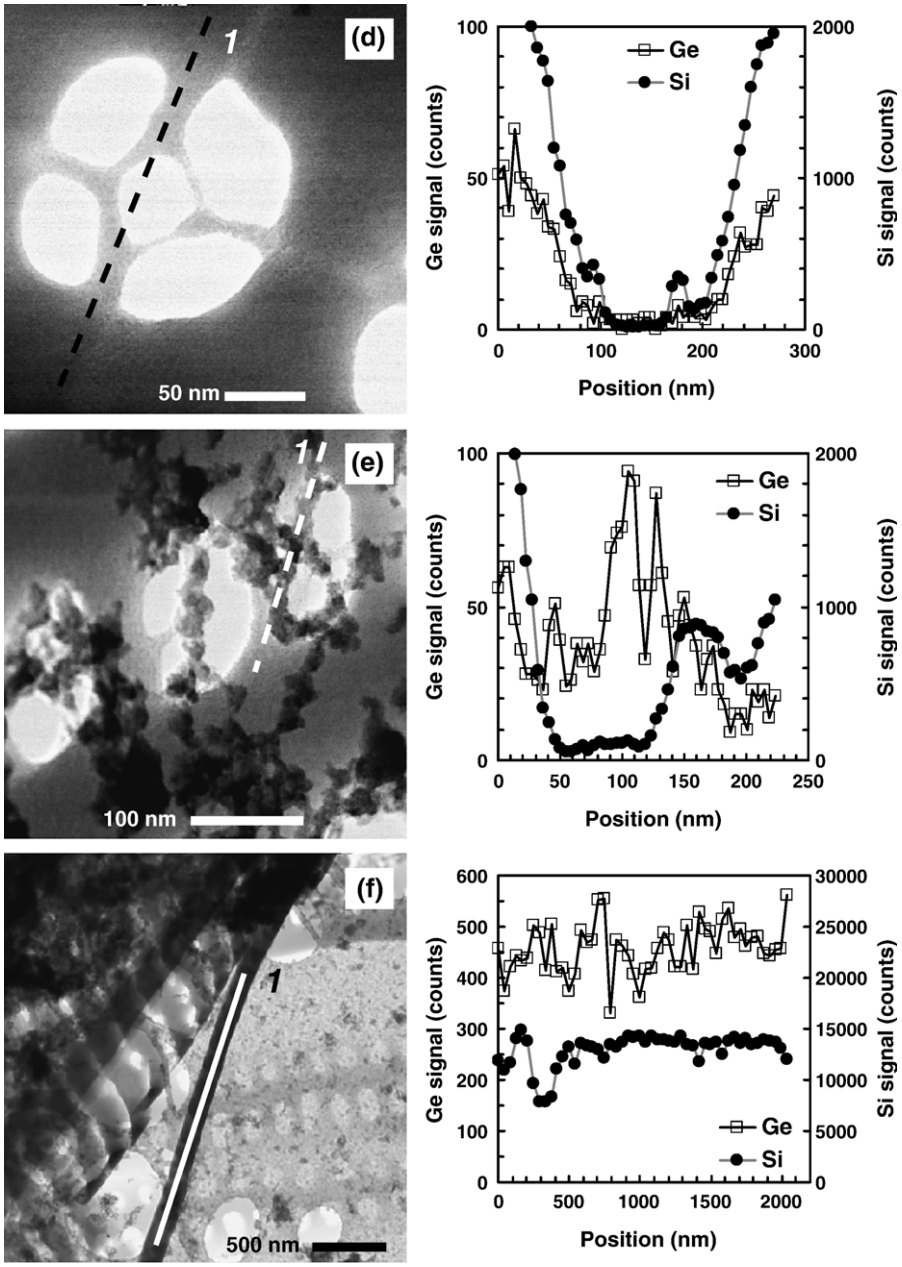

Fig. 7 (*continued*).

[36], whereas the chemical processes of frustule development are overviewed by Sumper and Brunner [10].

The two-stage photobioreactor cultivation strategy successfully incorporated a controlled amount of germanium into the biogenic silica frustule of the model marine diatom *Pinnularia* sp. and at the same time selectively altered the frustule morphology at the submicron and nanoscale. Many early reports have asserted that the addition of soluble germanium to diatom cell cultures inhibited cell growth and division, as germanium is not the natural substrate for these organisms [37–41]. However, from the bioprocessing perspective, germanium was simply an alternative substrate that was co-metabolized in the presence of silicon, the required substrate for cell division. Hence, a key feature of our bioprocessing strategy was the co-addition of soluble germanium with a sufficient amount of soluble silicon to support one cell division in Stage II (Fig. 2). During the single cell division in Stage II of the cultivation process, both Ge and Si were taken up into the cell (Figs. 3 and 4). When each cell divided, the new cell would contain a parent valve and a new valve of novel morphology containing germanium. Below, the rate processes of Si–Ge nanocomposite self-assembly that were directed by this bioprocessing strategy are discussed within the framework of the three stages of frustule development: soluble metal uptake, valve biofabrication, and cell division. A conceptual model of these processes is proposed in Fig. 8.

During Stage II of the cultivation process, both soluble silicon and germanium were transported into the silicon-starved diatom cell by a first-order process (Fig. 3) during the illumination phase of the photoperiod, consistent with the mechanism

Please cite this article as: C. Jeffryes et al., Mater. Sci. Eng. (2007), doi:10.1016/j.msec.2007.01.002

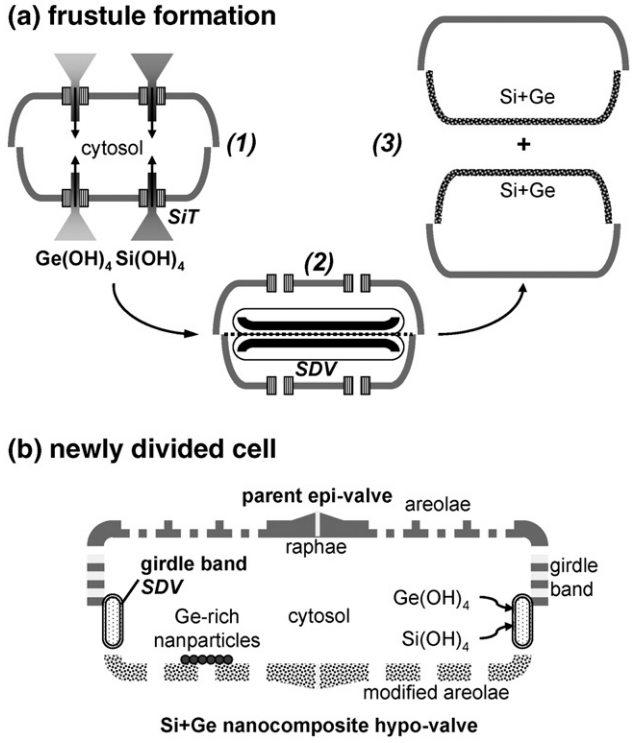

Fig. 8. Conceptual model for metabolic insertion of germanium into *Pinnularia* sp. frustule, as viewed from the proximal cross-section. (a) Cellular processes: (1) surge uptake of Si and Ge (SiT = Si transporter); (2) valve development; (3) cell division (SDV = silica deposition vesicle); (b) frustule from newly-divided cell from Stage II of cultivation, showing intracellular Ge located in the new *hypo*-valve, Ge-rich nanoparticles, the developing girdle band, and the cell cytosol.

of surge uptake during the G2 phase cell cycle. In fact, approximately two thirds of the silicon and germanium were taken up within 2 h, although cell doubling was not complete until 12 h into Stage II. It is well established that soluble silicon uptake into the diatom cell proceeds through a membrane-bound protein called the silicon transporter or SiT [42]. Furthermore, the rate of silicon uptake has a Michaelis–Menten dependence on the $Si(OH)_4$ form of soluble silicon [43]. Likewise, the $Ge(OH)_4$ form of soluble Ge would utilize the SiT for intracellular uptake. These results suggest that the intracellular uptake of Ge was not a rate-limiting step for metabolic insertion of germanium into the diatom frustule.

There was a limit to the extent of germanium uptake by *Pinnularia* sp. using the two-stage cultivation strategy described in this study. As long as Ge uptake during Stage II was complete, the culture growth parameters – specific growth rate, cell number yield, and biomass silicon content – were nominally constant as the Stage II initial Ge concentration was increased (Table 2, Fig. 4a). However, at a Stage II initial Ge concentration of 38 μmol/L, partial Ge efflux was evident and was tied to the dark phase of photoperiod (Fig. 3b), suggesting that Ge was ultimately inhibitory to the coupled machinery of frustule biosynthesis and cell division.

Germanium uptake into the diatom cell preceded its incorporation into the frustule biosilica. Germanium incorporation into the frustule was only possible if soluble Si was added to Stage II of the cultivation. If soluble Ge alone without Si was added to a diatom cell suspension culture, the cells initially took up the Ge. But shortly afterward the intracellular Ge did efflux back to the culture medium [29]. Comparison of the Ge contents in the cell mass and the isolated frustules (Fig. 4b, c) revealed that after 12 h of Stage II cultivation, cell division was complete, as were Si and Ge uptake into the cell. However, the incorporation of Ge into the frustule was not yet complete. Kröger and Wetherbee [36] reported that immediately after cell division, a second SDV specifically for the girdle band was formed just beneath the new *hypo*-valve. Therefore, it is possible that intracellular germanium in the new cell resulting from surge uptake by the parent cell continued to fortify its new frustule, particularly in the girdle band regions where a significant level of Ge in the frustule was observed (Fig. 7f). This process could be a rate-limiting step for metabolic insertion of germanium into the silica frustule.

Germanium was incorporated into the frustule silica and was not simply adsorbed or randomly precipitated onto the outer surface of the cell. Two lines of evidence support this conclusion. First, ICP analysis of the intact frustules isolated by aqueous hydrogen peroxide treatment of the diatom cell mass confirmed that Ge was present in the frustule (Fig. 4c). Aqueous hydrogen peroxide is known to dissolve germanium [44], and so only germanium imbedded into the silica as a germanium oxide would be resistant to dissolution. Second, the close correspondence of the elemental line scans for Si and Ge strongly suggested that germanium was alloyed into the silica frustule (Fig. 7), either in the form of Ge-oxide nanoclusters or germanosilicate (Si–O–Ge). A complimentary EDS elemental line scan through an imbedded cross-section of the diatom frustule was not performed, as it was assumed that the frustule was thin enough that a surface line scan would be sufficient. Further studies would also be needed to characterize putative Si–O–Ge structures by ^{29}Si MAS NMR [45] or Raman spectroscopy [46].

Metabolic insertion of germanium into the biogenic silica selectively altered frustule morphology (Figs. 6 and 7). The overall shape of the diatom was intact at the micron scale. However, at the submicron (100–1000 nm) and nanoscales (1–100 nm), the alloyed Si and Ge oxides resulting from metabolic insertion of Ge essentially thickened and at the same time "spread out" the biogenic silica, which in turn filled in or distorted the geometry of the *areolae*. This result is not surprising, since the intermediate range order of silicon and germanium oxides is quite different [47]. Furthermore, for amorphous silicon oxide [48] and amorphous germanium oxide [49], the bond length is 1.62 Å for Si–O vs. 1.74 Å for Ge–O, whereas the bond angle of Si–O–Si is 147° vs. 130° for Ge–O–Ge. One obvious consequence of this process is that metabolic insertion of Ge could be used to controllably reduce the pore aperture diameter and elongate the pore shape, perhaps into a slit-like geometry. Controlled alteration of nanoscale frustule pore aperture arrays by metabolic insertion of Ge has not been previously reported in diatoms. In addition to alterations in frustule morphology, there were germanium-rich pockets imbedded in the silica frustule and germanium-rich nanoparticles randomly littering the frustule surface (Fig. 7d, e), which might

Please cite this article as: C. Jeffryes et al., Mater. Sci. Eng. (2007), doi:10.1016/j.msec.2007.01.002

explain the appearance of dense cytoplasmic granules observed by Chiappino et al. [53] when the heterotrophic diatom *Nitzschia alba* was exposed to a mixture of soluble Si and Ge. Furthermore, silaffin peptides are known to promote the in vitro formation of amorphous germania structures [54]. One could speculate that these Ge-rich nanoclusters were fabricated by the SDV of the developing frustule and then sloughed off. The two-stage cultivation strategy used in this study was not capable of adding Ge to the organism in a way which could pattern the Si–Ge composite nanostructure.

As mentioned earlier, previous studies [37–41] showed that addition of soluble germanium to the diatom culture suspension inhibited cell division. We did not observe inhibition of cell division when a mixture of soluble silicon and germanium was fed to silicon-starved diatom cells, as long as the initial Si:Ge molar ratio in the Stage II culture medium was at least 14:1. Furthermore, none of these previous studies was verified by STEM–EDS if germanium was incorporated into the diatom frustule biosilica, and only one study provided evidence that frustule morphology was altered after diatom cells were exposed to a mixture of soluble silicon and germanium [53]. However, there is literature precedent for biological incorporation of germanium into the silica spicules of cultured sponge gemmule tissues [50–52]. Biological incorporation of germanium into the sponge spicule biosilica altered spicule tip morphology [52]. Furthermore, SEM-EDS studies confirmed the Ge was uniformly distributed within the spicule biosilica [50].

Estimation of the optoelectronic properties of *Pinnularia* sp. frustules bearing metabolically inserted germanium was beyond the scope of this study. In future work, we will characterize the photoluminescence and electroluminescence spectra of the novel, Si–Ge nanocomposite diatom frustules obtained from this study. We will also consider alternative bioreactor cultivation strategies under pH control in the attempt to more controllably manipulate the Si–Ge composite nanostructure and frustule microstructure.

Acknowledgement

This research was supported by the National Science Foundation (NSF) under Nanoscale Interdisciplinary Research Team (NIRT) award number BES-0400648.

References

[1] A. Kanjilal, J.L. Hansen, P. Gaiduk, A.N. Larsen, N. Cherkashin, A. Claverie, P. Normand, E. Kapelanaksis, D. Skarlatos, D. Tsoukalas, Appl. Phys. Lett. 82 (2003) 1212.
[2] M. Zacharias, P.M. Fauchet, Appl. Phys. Lett. 71 (1997) 380.
[3] J.G. Zhu, C.W. White, J.D. Budai, S.P. Withrow, Y. Chen, J. Appl. Phys. 78 (1995) 4386.
[4] Y. Negishi, S. Nagao, Y. Nakamura, A. Nakajima, J. Appl. Phys. 88 (2000) 6037.
[5] M. Zacharias, P.M. Fauchet, J. Non-Cryst. Solids 227–230 (1998) 1058.
[6] E. Dujardin, S. Mann, Adv. Mater. 14 (2002) 1.
[7] S. Zhang, Nat. Biotechnol. 21 (2003) 1171.
[8] M. Sarikaya, C. Tamerler, D.T. Schwartz, F. Baneyx, Annu. Rev. Mater. Res. 34 (2004) 373.
[9] Q. Sun, E.G. Vrieling, R.A. van Santen, N. Sommerdijk, Curr. Opin. Solid State Mater. Sci. 8 (2004) 111.
[10] M. Sumper, E. Brunner, Adv. Funct. Mater. 16 (2006) 17.
[11] J. Parkinson, R. Gordon, Trends Biotechnol. 17 (1999) 190.
[12] D.E. Morse, Trends Biotechnol. 17 (1999) 230.
[13] J. Bradbury, PLoS Biol. 2 (2004) 1512.
[14] P. Cohen, New Sci. 181 (2430) (2004) 26.
[15] R.W. Drum, R. Gordon, Trends Biotechnol. 21 (2003) 325.
[16] N. Kröger, R. Deutzmann, M. Sumper, Science 286 (1999) 1129.
[17] N. Kröger, R. Deutzmann, C. Bergsdorf, M. Sumper, PNAS 97 (2000) 14133.
[18] N. Kröger, S. Lorenz, E. Brunner, M. Sumper, Science 298 (2002) 584.
[19] R.R. Naik, P.W. Whitlock, F. Rodriguez, L.L. Brott, D.D. Glawe, S.J. Clarson, M.O. Stone, Chem. Commun. (2003) 238.
[20] M. Sumper, S. Lorenz, E. Brunner, Angew. Chem., Int. Ed. 42 (2003) 5192.
[21] N. Poulsen, N. Kröger, J. Biol. Chem. 279 (2004) 42993.
[22] M. Sumper, Angew. Chem., Int. Ed. 43 (2004) 2251.
[23] M. Xu, G.M. Gratson, E.B. Duoss, R.F. Shepherd, J.A. Lewis, Soft Matter 2 (2006) 205.
[24] T. Fuhrmann, S. Landwehr, M. El Rharbi-Kucki, M. Sumper, Appl. Phys., B 78 (2004) 257.
[25] L. De Stefano, I. Rendina, M. De Stefano, A. Bismuto, P. Maddelena, Appl. Phys. Lett. 87 (2005) 233902.
[26] K.S.A. Butcher, J.M. Ferris, M.R. Phillips, M. Wintrebert-Fouquet, J.W. Jong Wah, N. Jovanovic, W. Vyverman, V.A. Chepurnov, Math. Sci. Eng. C 25 (2005) 658.
[27] S. Shian, Y. Cai, M.R. Weatherspoon, S.M. Allan, K.H. Sandhage, J. Am. Ceram. Soc. 89 (2006) 694.
[28] N.L. Rosi, C.S. Thaxton, C.A. Mirkin, Angew. Chem., Int. Ed. 43 (2004) 5500.
[29] G.L. Rorrer, C.-H. Chang, S.-H. Liu, C. Jeffryes, J. Jiao, J.A. Hedberg, J. Nanosci. Nanotechnol. 5 (2005) 41.
[30] S.A. Crawford, M.J. Higgins, P. Mulvaney, R. Wetherbee, J. Phycol. 37 (2001) 543.
[31] K. Krammer, Pinnularia: eine Monographie der europäischen Taxa, J. Cramer, Berlin, 1992.
[32] K.A. Fanning, M.E.Q. Pilson, Anal. Chem. 45 (1973) 136.
[33] C.L. Luke, M.E. Campbell, Anal. Chem. 28 (1956) 1273.
[34] Z. Marczenko, Spectrophotometric Determination of the Elements, Ellis Horwood Ltd./John Wiley and Sons, New York, 1976.
[35] V. Martin-Jézéquel, M. Hildebrand, M.A. Brzeziniski, J. Phycol. 36 (2000) 821.
[36] N. Kröger, R. Wetherbee, Protist 151 (2000) 263.
[37] J. Lewin, Phycologia 6 (1966) 1.
[38] F. Azam, B.B. Hemmingsen, B.E. Volcani, Arch. Mikrobiol. 92 (1973) 11.
[39] D. Werner, M. Petersen, Z. Pflanzenphysiol. 70 (1973) 54.
[40] F. Azam, B.E. Volcani, Arch. Microbiol. 101 (1974) 1.
[41] C.W. Mehard, C.W. Sullivan, F. Azam, B.E. Volcani, Physiol. Plant. 30 (1974) 265.
[42] M. Hildebrand, in: E. Baeuerlein (Ed.), Biomineralization: from Biotechnology to Medical Application, Wiley-VCH, Weinheim, 2000, p. 171.
[43] Y. Del Amo, M.A. Brzezinski, J. Phycol. 35 (1999) 1162.
[44] N. Cerniglia, P. Wang, J. Electrochem. Soc. 109 (1962) 508.
[45] A. Gendron-Badou, T. Coradin, J. Maquet, F. Fröhlich, J. Livage, J. Non-Cryst. Solids 316 (2003) 331.
[46] S.K. Sharma, D.W. Matson, J.A. Philpotts, T.L. Roush, J. Non-Cryst. Solids 68 (1984) 99.
[47] S. Kohara, K. Suzuya, J. Phys. Condens. Mat. 17 (2005) S77.
[48] D.A. Keen, M.T. Dove, J. Phys. Condens. Mat. 11 (1999) 9263.
[49] D.E. Sayers, E.A. Stern, F.W. Lytle, Phys. Rev. Lett. 35 (1975) 584.
[50] E.I. Davie, T.L. Simpson, R. Garrone, Biol. Cell 48 (1983) 191.
[51] T.L. Simpson, R. Garrrone, M. Mazzorana, J. Ultrastruct. Res. 85 (1983) 159.
[52] T.L. Simpson, M. Gil, R. Connes, J.-P. Diaz, J. Paris, J. Morphol. 183 (1985) 117.
[53] M.L. Chiappino, F. Azam, B.E. Volcani, Protoplasma 93 (1977) 191.
[54] M.B. Dickerson, R.R. Naik, M.O. Stone, Y. Cal, K.H. Sandhage, Chem. Commun. (2004) 1776.

Please cite this article as: C. Jeffryes et al., Mater. Sci. Eng. (2007), doi:10.1016/j.msec.2007.01.002